



**HAL**  
open science

## Acoustic characterization of Silica aerogel clamped plates for perfect absorption

A. Geslain, J.-P. Groby, V. Romero-Garcia, F. Cervera, J. Sánchez-Dehesa

► **To cite this version:**

A. Geslain, J.-P. Groby, V. Romero-Garcia, F. Cervera, J. Sánchez-Dehesa. Acoustic characterization of Silica aerogel clamped plates for perfect absorption. *Journal of Non-Crystalline Solids*, 2018, 499, pp.283-288. 10.1016/j.jnoncrysol.2018.07.021 . hal-02366101

**HAL Id: hal-02366101**

**<https://hal.science/hal-02366101>**

Submitted on 15 Nov 2019

**HAL** is a multi-disciplinary open access archive for the deposit and dissemination of scientific research documents, whether they are published or not. The documents may come from teaching and research institutions in France or abroad, or from public or private research centers.

L'archive ouverte pluridisciplinaire **HAL**, est destinée au dépôt et à la diffusion de documents scientifiques de niveau recherche, publiés ou non, émanant des établissements d'enseignement et de recherche français ou étrangers, des laboratoires publics ou privés.

# Acoustic characterization of Silica aerogel clamped plates for perfect absorption

A. Geslain

*DRIVE EA1859, Univ. Bourgogne Franche Comté, F58000, Nevers France.*

J.-P. Groby, V. Romero-García

*Laboratoire d'Acoustique de l'Université du Mans, L'Université Nantes Angers Le Mans, Université du Mans, UMR CNRS 6613, Avenue Olivier Messiaen, 72085 Le Mans, France.*

F. Cervera, J. Sánchez-Dehesa

*Wave Phenomena Group, Departamento de Ingeniería Electrónica, Universitat Politècnica de València, Camino de vera s/n (Edificio 7F), E-46022 València, Spain*

---

## Abstract

A multiobjective optimization procedure is employed to retrieve the viscoelastic parameters of silica aerogel clamped plates. This retrieval method preserves the aerogel sample integrity and, in contrast to the existing ones, relies on the minimization of two different cost functions. The first one, namely  $J_1$ , is related to the reflective properties of clamped plates backed by a rigid cavity, while the second one, namely  $J_2$ , concerns both the reflectance and transmittance spectra measured in transmission configuration. The recovered parameters are in agreement with previously reported values in the literature. In addition, they are also supported by designing structures for perfect absorption (100 % of absorption), which has been validated experimentally. Aerogel plates can be therefore used as innovative building units of artificial structures for the broadband absorption of sound.

*Keywords:* Aerogel, Acoustics, Mechanical characterization, Genetic algorithm

---

## 1. Introduction

1 Silica aerogels have been mainly developed for thermal and acoustic insulation purposes [1, 2]. Therefore, their manufacturing process has been widely studied to improve their bulk properties and they present an extremely low density [3], an ultra low thermal conductivity [4], and a subsonic sound velocity [5, 6]. The extremely low static density is directly related to their high porosities. The frame of silica aerogel effectively consists of an assembly of connected small cross-sections beam-like elements resulting from fused nanoparticles. This particular assembly additionally provides silica aerogel a very low elastic stiffness when compared to rigid silica structure of identical porosity [6]. Silica aerogels are then nanoporous lightweight materials [2]. Beyond these soft bulk material properties, silica aerogel plates or membranes are excellent candidates to design original acoustic metamaterials, because they exhibit subwavelength resonances and present efficient absorption capabilities [7].

21 Recently, membrane-type metamaterials have shown an increasing interest to control acoustic waves. While a single membrane presents negative mass density [8] as well as may be used as a perfect subwavelength absorber [9, 10], the periodic arrangement of plates combined with other kind of resonators presents single and double negativity [11]. More recently, periodic arrangement of clamped plates has been used to control the harmonic generation [12] and the solitary wave generation in the nonlinear acoustic regime [13].

31 The characterization of the elastic properties of the silica aerogel plates is therefore primordial to design efficient aerogel-based acoustic metamaterials. Two types of test have been yet proposed to characterize their elastic properties: mechanical destructive tests and ultrasonic non-destructive tests. On the one hand, Woignier *et al.* [14, 15, 16] used 3-point bending and uniaxial compression while Haj-Ali *et al.* [17] used digital image correlation technique to determine the mechanical behavior of aerogel. On the other hand, ultrasonic tests

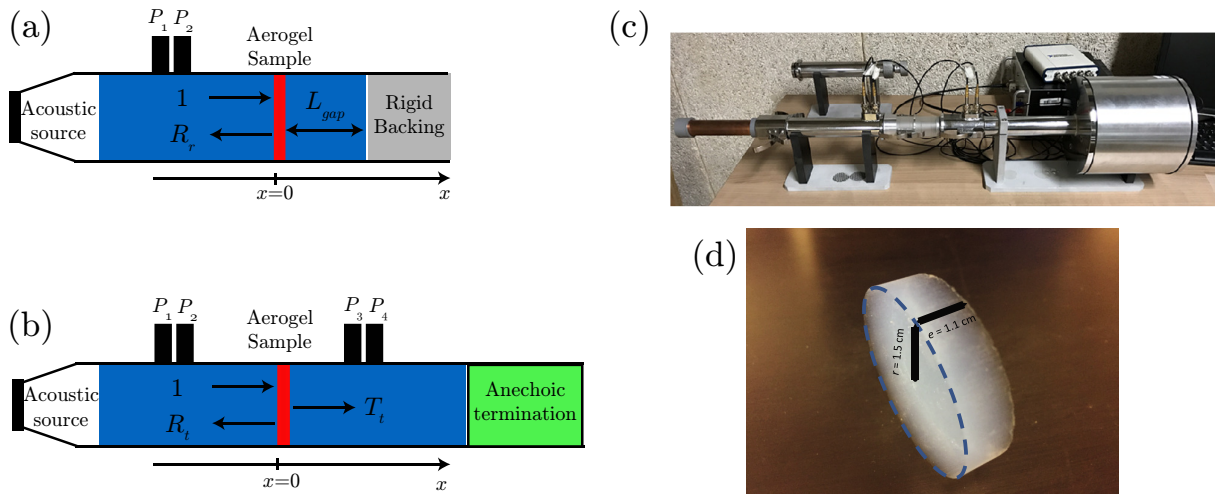


Figure 1: Reflection and transmission configurations and experimental set-up. (a) acoustic reflection configuration to determine reflection coefficient from the evaluated pressure  $P_1$ ,  $P_2$ . (b) acoustic transmission problem to assess reflection and transmission coefficients from the pressures  $P_1$ ,  $P_2$ ,  $P_3$ ,  $P_4$ . (c) Acoustic impedance tube mounted for the experimental characterization of the transmission problem. (d) Photograph of a Silica aerogel plate with thickness  $e = 1.1$  cm and radius  $r = 1.5$  cm.

[5, 6, 18, 19] provide acoustic properties but are limited in terms of frequencies and by definition do not provide information in the audible regime.

This work aims at providing the viscoelastic properties of silica aerogel plates in the audible frequency range thanks to a novel signal processing method based on usual impedance tube measurements which have the advantage to preserve the sample integrity. The silica aerogel, being nanoporous, can be approximated by a viscoelastic material in this low frequency regime; i.e. in the audible frequency range. In this work we also show that clamped plates of silica aerogel can be used to design ultralight acoustic metamaterials for the perfect absorption of sound.

The article is divided in four Sections. In Section 2, the proposed method to retrieve the elastic properties is presented. A genetic optimization algorithm is used with two objective (or cost) functions to estimate Young modulus, loss factor, Poisson's ratio and mass density of the sample. The two objective functions arise from two complementary acoustic configurations: the reflection problem, where the aerogel membrane is backed with a rigid cavity, and the transmission problem. Section 3 make use of the recovered parameters to derive the perfect absorption (PA) condition [9, 20] (i.e.  $\alpha = 1$ , where  $\alpha$  is the acoustic absorption) when the silica-aerogel plate is backed by a rigid cavity of a specific length. By varying the cavity length from 0.5 cm to 6.5 cm, the positions of both zeros and poles of the reflection coefficients are studied in the complex frequency domain.

Section 4 provides the concluding remarks and comments.

## 2. Acoustic characterization of the silica aerogel plate mechanical properties

The characterization of the viscoelastic properties of the silica aerogel plate is based on the analysis of data acquired in the two configurations shown in Fig. 1. In the first one, depicted in Fig. 1(a), the reflection coefficient of the aerogel plate when rigidly backed with an air cavity is measured. In the second one, depicted in Fig. 1(b), both the reflection and transmission coefficients of the aerogel plate in a transmission problem are measured. In addition, Fig. 1(c) shows a photograph of the experimental setup for the characterization.

In this Section, we present the retrieval procedure which consists in minimizing the difference between the experimental and the theoretical coefficients.

### 2.1. Direct modeling

Assuming a Kirchhoff-Love plate [21], the transverse displacement  $w_s$  satisfies the equation of motion

$$D\nabla^4 w_s + e\rho \frac{\partial^2 w_s}{\partial t^2} = 0, \quad (1)$$

where  $e$  is the plate thickness,  $\rho$  is the plate density and  $D$  is the flexural rigidity.  $D = \frac{Ee^3}{12(1-\nu^2)}$ , where  $E$  is the Young modulus and  $\nu$  is the Poisson coefficient. Considering the temporal convention  $e^{i\omega t}$ , with

96  $\omega$  the angular frequency, the silica aerogel viscoelastic 133  
 97 behavior implies a complex Young modulus of the 134  
 98 form  $E = E_r(1 + i\eta\omega)$ , where  $E_r$  is the real part of the 135  
 99 Young modulus and  $\eta$  is the loss factor. Assuming a 136  
 100 sub-wavelength regime, the silica aerogel disk is con- 137  
 101 sidered as a punctual resonant element. The acoustic 138  
 102 impedance  $Z_p$  of a clamped circular cross-section plate 139  
 103 was derived [7] and takes the form,

$$104 \quad Z_p = \frac{-i\omega\rho e I_1(k_p r)J_0(k_p r) + J_1(k_p r)I_0(k_p r)}{S I_1(k_p r)J_2(k_p r) - J_1(k_p r)I_2(k_p r)}, \quad (2)$$

105 where  $S = \pi r^2$  is the cross-section surface of the plate,  
 106  $J_n$  and  $I_n$  are the regular and modified Bessel functions  
 107 of the first kind of order  $n \in \{0, 1, 2\}$  and  $k_p^2 = \omega \sqrt{\rho e/D}$   
 108 is the plate wavenumber.

109 In the impedance tube, the aerogel clamped plate  
 110 acoustically behaves as a point resonator mounted in  
 111 series, implying sound velocity continuity and pressure  
 112 discontinuity. Therefore, the clamped plate can be re-  
 113 presented by a matrix  $M_p$  when using the transfer matrix  
 114 method, [22] which reads as

$$115 \quad [M_p] = \begin{bmatrix} M_{p11} & M_{p12} \\ M_{p21} & M_{p22} \end{bmatrix} = \begin{bmatrix} 1 & Z_p \\ 0 & 1 \end{bmatrix}. \quad (3)$$

116 The reflection and transmission coefficients for this  
 117 symmetric and reciprocal transmission problem are then  
 118 directly obtained from the elements of  $M_p$  as, [22]

$$119 \quad T = \frac{2e^{ikL}}{M_{p11} + M_{p12}/Z_t + Z_t M_{p21} + M_{p22}}, \quad (4)$$

$$120 \quad R = \frac{M_{p11} + M_{p12}/Z_t - Z_t M_{p21} - M_{p22}}{M_{p11} + M_{p12}/Z_t + Z_t M_{p21} + M_{p22}}, \quad (5)$$

121 where  $Z_t = \rho_t c_t / S$  is the impedance of the surround-  
 122 ing medium, i.e. in our case the effective fluid occupy-  
 123 ing in the impedance tube,  $S$  is the characteristic cross-  
 124 sectional area of the tube,  $k$  is the wavenumber in the  
 125 air and  $L$  is the length of the sample, in our case  $L = e$ .  
 126 Viscous and thermal losses are effectively accounted for  
 127 in the tube thanks to the formulae provided by Stinson  
 128 [23].

129 The aerogel plate system being symmetric and recip-  
 130 erocal, the modeled coefficients in the transmission prob-  
 131 lem are given by,

$$132 \quad T_{mod}^t = \frac{2}{2 + Z_p/Z_t}, \quad (6)$$

$$133 \quad R_{mod}^t = \frac{Z_p/Z_t}{2 + Z_p/Z_t}.$$

134 In the reflection problem, the system is composed of  
 135 an aerogel plate in front of a closed cavity. In this case,

the transfer matrix method reads as,

$$136 \quad \begin{bmatrix} P \\ V \end{bmatrix}_{x=0} = [M_p][M_c] \begin{bmatrix} P \\ 0 \end{bmatrix}_{x=L_{gap}}, \quad (7)$$

with the propagation matrix  $M_c$  given by

$$137 \quad [M_c] = \begin{bmatrix} \cos(k_t L_{gap}) & iZ_t \sin(k_t L_{gap}) \\ i \sin(k_t L_{gap})/Z_t & \cos(k_t L_{gap}) \end{bmatrix}, \quad (8)$$

138 where  $k_t$  is the wavenumber in the closed cavity (ac-  
 139 counting for viscothermal losses) and  $L_{gap}$  is the cavity  
 140 length. The reflection coefficient is thus,

$$141 \quad R_{mod}^r = \frac{Z_{syst} - Z_t}{Z_{syst} + Z_t}, \quad (9)$$

where  $Z_{syst} = P_{x=0}/V_{x=0}$  is the system impedance.

## 142 2.2. Measurements of the reflection and transmission 143 coefficients

144 The reflection and transmission coefficients in each  
 145 configuration are measured following the recovery of the  
 146 scattering matrix elements as explained for example  
 147 in Ref. [24]. In the reflection configuration, the  
 148 two acoustic pressures,  $P_1$  and  $P_2$ , are measured by the  
 149 two microphones located upstream from the material to  
 150 extract the frequency dependent experimental reflection  
 151 coefficient  $R_{exp}^r(f)$  (where  $f$  is the frequency). In the  
 152 transmission problem, Fig. 1(b), the four acoustic pres-  
 153 sures,  $P_1, P_2, P_3$ , and  $P_4$ , are measured by a pair of mi-  
 154 crophones located upstream and downstream from the  
 155 material to obtain the experimental reflection and trans-  
 156 mission coefficients  $R_{exp}^t(f)$  and  $T_{exp}^t(f)$  assuming the  
 157 sample is symmetric.

158 The experimental setup is depicted in Fig. 1(c). The  
 159 diameter of the impedance tube is  $d_t = 3$  cm. The ex-  
 160 perimental data are acquired with an excitation of 3000  
 161 sine functions equally spaced between 20 Hz and 6000  
 162 Hz. Four 1/4 inch microphones are flush mounted, con-  
 163 nected to a spectral analyser and measure the acoustic  
 164 pressure. Each measurement is averaged 30 times to  
 165 obtain the transfert function between the microphones.  
 166 The aerogel samples are presented in Fig. 1(d).

## 167 2.3. Retrieval procedure: Multiobjective optimization

168 Decisions on optimal design in many scientific or en-  
 169 gineering areas require a compromise between different  
 170 objectives (or cost functions). It is therefore natural to  
 171 look for the best solution to each of these cost functions.  
 172 However, an improvement in one of the cost function  
 173 can lead to a deterioration in the other ones if some cost  
 174 functions are conflicting with the other. The absence of

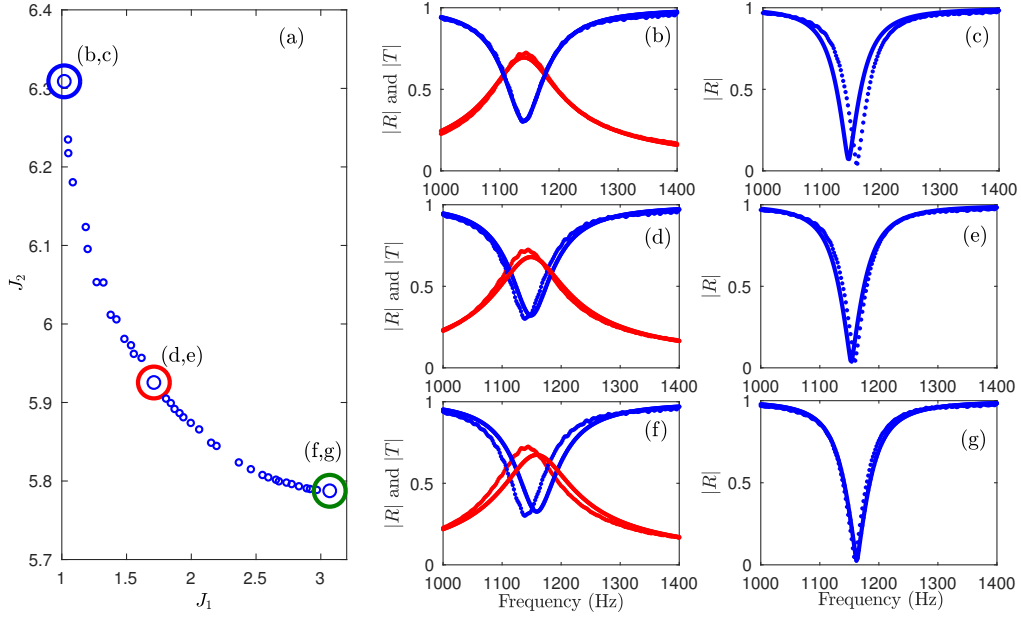


Figure 2: (a) Pareto front of the two objective functions  $J_1$  and  $J_2$ . Big blue (red) [green] circle in (a) represents the Point 1 [2] [3] in Table 1. The reconstructed reflection and transmission coefficients for the transmission problem for this solution are shown in (b) [(d)] [(f)] while the reconstructed reflection coefficient for the reflection problem is shown in (c) [(e)] [(g)]. Full lines represent the theoretical coefficients while dotted lines represents experimental results.

175 a single optimal solution is effectively a difficulty. Multi-  
 176 multiobjective optimization problems enable to avoid this  
 177 issue. The optimal solution consists in a set  $\Theta_p$  named  
 178 Pareto set [25]. The main characteristic of this set is  
 179 that none of these elements are better than the others for  
 180 some of the objectives. This means that all solutions are  
 181 optimal in some sense.

182 In this Section we define the cost functions that are  
 183 minimized by the multiobjective algorithm to retrieve  
 184 the viscoelastic parameters of the aerogel plates, as well  
 185 as the criteria chosen to identify the best solution and  
 186 analyze the Pareto set. For the optimization problem,  
 187 our approach is based on the use of evolutionary algo-  
 188 rithms, which enable the simultaneous generation of  
 189 several elements of the Pareto set in parallel and in a single  
 190 run. Among these evolutionary algorithms, genetic  
 191 algorithms, which are inspired by biological evolution  
 192 (crossover, mutation, recombination and selection), are  
 193 used [26]. The individuals of the genetic algorithm are  
 194 coded by chromosomes of the form,  $(\rho, \nu, E, \eta)$ . An  
 195 initial population (a set of possible solutions) evolves  
 196 by applying genetic operators that combine the charac-  
 197 teristics of some of the individuals of the population.  
 198 At each iteration, the population changes and adapts to  
 199 converge to the optimal solution  $\Theta_p$ .

### 2.3.1. The cost functions

200 To retrieve the viscoelastic properties of the aerogel  
 201 plate, two cost functions are defined. The two objective  
 202 functions  $J_1$  (transmission problem) and  $J_2$  (reflec-  
 203 tion problem) are composed of the  $L_2$  norms of the differ-  
 204 ences between the experimental and theoretical acoustic  
 205 reflection and transmission coefficients over a range of  
 206 frequencies centered on the resonance frequency system  
 207 considered,  
 208

$$J_1 = \sum_{f=f_1}^{f_2} \|R_{exp}^t(f) - R_{mod}^t(\rho, \nu, E, \eta, f)\|^2 + \sum_{f=f_1}^{f_2} \|T_{exp}^t(f) - T_{mod}^t(\rho, \nu, E, \eta, f)\|^2, \quad (10)$$

$$J_2 = \sum_{f=f_1}^{f_2} \|R_{exp}^r(f) - R_{mod}^r(\rho, \nu, E, \eta, f)\|^2, \quad (11)$$

209 where  $R_{exp}^t, T_{exp}^t$  ( $R_{mod}^t, T_{mod}^t$ ) are the experimental (re-  
 210 spectively modeled) reflection and transmission coeffi-  
 211 cients in the transmission problem, and  $R_{exp}^r$  ( $R_{mod}^r$ ) is  
 212 the experimental (respectively modeled) reflection co-  
 213 efficient in the reflection problem. In the summations  
 214  $f_1 = 1124$  Hz and  $f_2 = 2324$  Hz. Each experimen-  
 215 tal coefficients were measured several times to check

216 the measurement repeatability. The mechanical prop-  
 217 erties of the silica aerogel plate being independent of  
 218 the length of the backing cavity, we chose without loss  
 219 of generality and for convenience of our experimental  
 220 setup, the gap thickness  $L_{gap} = 0.5$  cm for the reflection  
 221 problem [see Fig. 1(a)].

### 222 2.3.2. Solutions: Pareto front

223 Figure 2(a) shows the Pareto fronts of optimization  
 224 procedure results. Each open circle in the Pareto front  
 225 represents a solution with a different set of param-  
 226 eters  $\{\rho, \nu, E_r, \eta\}$ . The position of the solution in the  
 227 Pareto front provides information on the accuracy of  
 228 the retrieval procedure by using the two configurations  
 229 previously described. The range of variation of the  
 230 cost function  $J_2$  is smaller than that of  $J_1$  (see Fig.  
 231 2(a)). Therefore, the parameters are less sensitive to  
 232 the reflection problem than to the transmission prob-  
 233 lem. In order to compare their accuracy, three solu-  
 234 tions are given in Table 1. These three solution are re-  
 235 spectively highlighted in the Figure 2(a) with blue, red  
 236 and green circles. Among all the solutions, the point  
 237  $(J_1, J_2) = (1.027, 6.308)$  [ $(J_1, J_2) = (3.077, 5.786)$ ] rep-  
 238 represents the best [wrong] solution for the objective  $J_1$ ,  
 239 i.e. for the transmission problem, and the worst [best]  
 240 solution for the objective  $J_2$ , i.e. for the reflection prob-  
 241 lem. We can clearly see in Figs. 2(b,c) [Figs. 2(f,g)]  
 242 that the differences between the reflection and transmis-  
 243 sion coefficients obtained for the transmission [reflec-  
 244 tion] problem are smaller than the ones obtained for the  
 245 reflection [transmission] problem for this solution. The  
 246 corresponding estimated parameters are summarized in  
 247 the Table 1. The retrieval procedure provides relatively  
 248 identical values of  $\{\rho, E_r, \eta\}$  at both points. This means  
 249 the transmission problem is enough to estimate these  
 250 three parameters. In order to estimate  $\nu$ , the multiob-  
 251 jective optimization procedure accounting additionally  
 252 for the reflection problem should be considered.

253 In the opposite, the point  $(J_1, J_2) = (1.719, 5.924)$   
 254 represents the solution with the minimal distance to the  
 255 origin of coordinates, showing that the differences be-  
 256 tween the theory and the experiments for both problems  
 257 are similar (see Fig. 2(d,e)). As a consequence, the cri-  
 258 terium to choose the best solution is based on the mini-  
 259 mal distance to the origin of coordinates, and this point  
 260 is chosen as the solution of our problem. The retrieved  
 261 viscoelastic parameters are given in Tab. 1 and their val-  
 262 ues are in agreement with others previously reported in  
 263 the literature [27, 28].

264 In order to further support the viscoelastic param-  
 265 eters provided by the optimization problem, results of  
 266 reflection problems with different values of the cavity

Table 1: Optimal aerogel mechanical parameters of the three selected points in Fig. 2.

	$\rho$ ( $\text{kg}\cdot\text{m}^{-3}$ )	$\nu$	$E_r$ (k Pa)	$\eta$ ( $10^{-6}$ )
Point 1	80	0.09	197.51	4.19
Point 2	80	0.12	197.92	4.47
Point 3	80	0.17	197.99	4.50

267 thickness  $L_{gap} = [0.5, 1, 6.5]$  cm are compared to mea-  
 268 surements. Results of the absolute value and the phase  
 269 of the reflection coefficients are respectively shown in  
 270 Fig. 3(a) and 3(b). Continuous and dotted lines repre-  
 271 sent respectively the theoretical values and experimen-  
 272 tal results respectively. The theoretical predictions and  
 273 experimental data are in good agreement, giving sup-  
 274 port to the viscoelastic parameters estimated by the pro-  
 275 posed optimization procedure and also validating both  
 276 the measurement and the model approach.

### 277 3. Critical coupling condition and perfect absorp- 278 tion

279 The absorption properties of a system composed of  
 280 the silica aerogel plate is studied making use of the pre-  
 281 viously estimated viscoelastic properties. The aerogel  
 282 plate behaves as a viscoelastic clamped plate with in-  
 283 trinsic losses. The combination of an elastic plate with  
 284 a back closed cavity, as shown in Fig. 1(a), can be  
 285 analyzed as an open lossy resonator. In this case, the  
 286 resonator presents two types of losses, the energy leak-  
 287 age of the open resonator and the intrinsic losses of  
 288 the system. Recently, the design of perfect absorbers  
 289 for acoustic wave has received an increasing interest  
 290 [10, 9, 29, 20, 30]. The perfect absorption (PA) con-  
 291 dition (*i.e.*  $\alpha = 1$ , where  $\alpha$  is the acoustic absorption co-  
 292 efficient) is related to the exact counterbalance between  
 293 the energy leakage of the system and the dissipated en-  
 294 ergy by the inherent losses [20], which is known as the  
 295 critical coupling condition. In this Section we show the  
 296 efficiency of systems based on silica aerogel plates to  
 297 perfectly absorb the acoustic energy.

298 In order to provide insights to the perfect absorption  
 299 process, the reflection coefficient of an aerogel plate  
 300 backed by a closed cavity is analyzed in the complex  
 301 frequency plane for different cavity lengths. The cavity  
 302 length  $L_{gap}$  varies between 0.5 cm and 6.5 cm. In the  
 303 present problem, the eigenvalue of the scattering ma-  
 304 trix reduces to the reflection coefficient. The measured

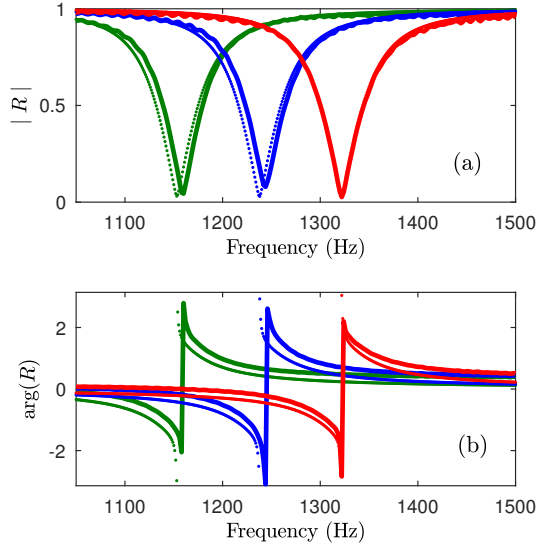


Figure 3: Comparison of the experimental reflection coefficient (circles) and the reconstructed reflection coefficient (solid lines)  $[R_{exp}^r, R_{mod}^r]$  for the back cavity length  $L_{gap} = [0.5, 1, 6.5]$  cm [red, blue and green lines and symbols respectively]

. Aerogel mechanical parameters  $[\rho = 80 \text{ kg/m}^3, \nu = 0.12, E_r = 197.92 \text{ kPa}, \eta = 4.47 \cdot 10^{-6}]$ . (a) absolute value of the reflection coefficients. (b) phase of the reflection coefficient.

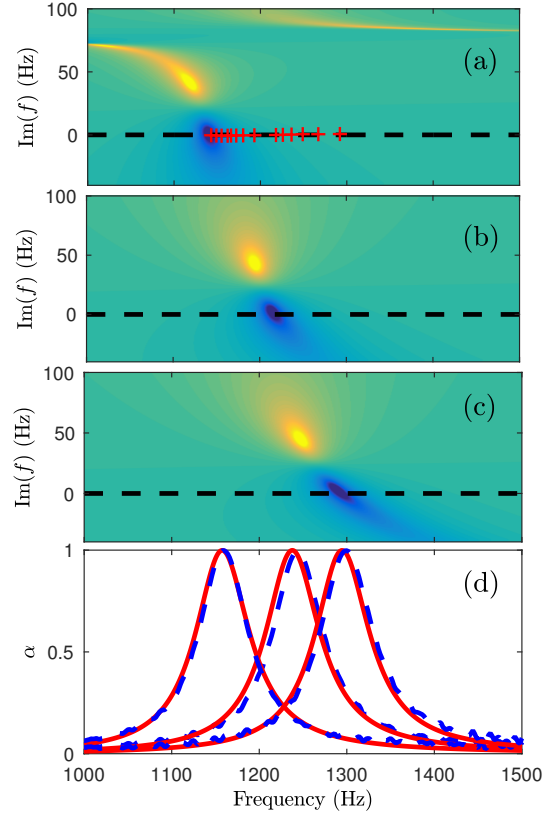


Figure 4: (a)-(c) Representation of the  $\log_{10}(|R|^2)$  (color scale), in the complex frequency plane for the configurations with  $L_{gap} = [0.5, 1, 6.5]$  cm respectively. In (a) red crosses represent the complex frequency of the zero of  $|R|$  in the complex frequency plane for the configurations  $L_{gap} = [0.5, 0.6, 0.7, 0.8, 0.9, 1.0, 1.5, 2.0, 2.5, 3.0, 3.5, 4.5, 5.5, 6.5]$  cm. (d) Comparison of the absorption coefficients,  $\alpha$ , for  $L_{gap} = [0.5, 1, 6.5]$  cm (in solid line theoretical reconstructed coefficients and in dashed line experimental results).

305 reflection coefficient corresponds to the one calculated  
 306 along the real frequency axis. Therefore, the perfect  
 307 absorption condition occurs in the complex frequency  
 308 plane when the zero of the reflection coefficient crosses  
 309 the real frequency axis [9, 20].

310 Figures 4(a), (b) and (c) show the reflection coefficient  
 311 in the complex frequency plane for the configuration  
 312 with  $L_{gap} = [0.5, 1, 6.5]$  cm respectively. For  
 313 these three configurations, the zero of the reflection  
 314 coefficient shifts at low frequencies when cavity length  
 315 increases and, more importantly, it stands on the real  
 316 frequency axis. Moreover, the zero of the reflection  
 317 coefficient of each of these configurations is located exactly  
 318 on the real frequency axis (red crosses in Fig. 4(a)),  
 319 meaning that all these configurations present perfect  
 320 absorption. It is remarkable that the frequency at which  
 321 perfect absorption is obtained is tunable in a broad range  
 322 of frequencies by tuning  $L_{gap}$ .

323 Perfect absorption was experimentally verified. Red  
 324 and blue dashed lines in Fig. 4(d) show the theoretical  
 325 reconstructed predictions and the experimental results  
 326 respectively. We can see that the frequency at which  
 327 perfect absorption is obtained corresponds to the situation  
 328 in which the zero of the reflection coefficients is

329 located on the real frequency axis. The agreement between  
 330 the theory and the experiments is very good and makes  
 331 aerogel plate backed by a closed cavity as an innovative  
 332 artificial structures for acoustic absorption purpose.  
 333

#### 334 4. Summary

335 A novel signal processing method for retrieving the  
 336 viscoelastic properties of a silica aerogel clamped plate  
 337 is presented. This method is based on a genetic algorithm  
 338 optimization with two objective functions resulting from  
 339 two acoustic configurations, a reflection problem and a  
 340 transmission problem in an acoustic impedance tube. The  
 341 two objective functions are com-

posed of the  $L_2$  norms of the differences between the experimental and modeled acoustic problems around the plate resonance frequency. The estimated aerogel viscoelastic properties are  $\rho = 80 \text{ kg/m}^3$ ,  $\nu = 0.12$ ,  $E_r = 197.92 \text{ kPa}$ ,  $\eta = 4.47 \cdot 10^{-6}$ . These values are close to those previously reported in the literature. The main advantages of the present method is that the aerogel silica sample is undamaged and due to the genetic algorithm process the estimated viscoelastic properties satisfy identically the transmission and reflection problems in the audible frequency range. Once the viscoelastic properties of the silica aerogel plate are characterized, the perfect absorption condition (*i.e.*  $\alpha = 1$ , with  $\alpha$  is the acoustic absorption) is derived for a system consisting in an aerogel plate backed by a rigid cavity. It is shown that such a system possess the ability to perfectly absorb sound over a wide range of cavity length, and therefore over a wide range of possible frequency. The absorptive properties of aerogel are encouraging and can be applied to design more complex artificial structures (metasurfaces) for the broadband absorption of sound.

## 5. Acknowledgments

This article is based upon work from COST Action DENORMS CA15125, supported by COST (European Cooperation in Science and Technology). The authors are grateful to the French ANR project Metaudible (ANR-13-BS09-0003) and to RFI Le Mans Acoustique (Région Pays de la Loire) PAVNat and Aerogel projects. F.C and J.S-D. acknowledge the partial support by the Ministerio de Economía y Competitividad of the Spanish Government and the European Union "Fondo Europeo de Desarrollo Regional (FEDER)" through project No. TEC2014-53088-C3-1-R.

- [1] L. W. Hrubesh, "Aerogel applications", J. Non-Cryst. Solids **225**, 335 (1998).
- [2] M. Schmidt, F. Schwertfeger, "Applications for silica aerogel products", J. Non-Cryst. Solids **225**, 364–368 (1998).
- [3] M. Li, H. Jiang, D. Xu, O. Hai and W. Zheng, "Low density and hydrophobic silica aerogels dried under ambient pressure using a new co-precursor method", J. Non-Cryst. Solids **452**, 187-193 (2016).
- [4] Q. Xu, H. Ren, J. Zhu, Y. Bi, Y. Xu and L. Zhang, "Facile fabrication of graphite-doped silica aerogels with ultralow thermal conductivity by precise control", J. Non-Cryst. Solids **469**, 14-18 (2017).
- [5] V. Gibiat, O. Lefeuvre, T. Woignier, J. Pelous and J. Phalippou "Acoustic properties and potential applications of silica aerogels", J. Non-Cryst. Solids **186**, 244-255, (1995).
- [6] M. Gronauer and J. Fricke, "Acoustic properties of microporous SiO<sub>2</sub>-aerogel", Acta Acust united Ac. **59**, 177 (1986).
- [7] M. Guild, V.M. García-Chocano, J. Sánchez-Dehesa, T.P. Martin, D.C. Calvo, and G.J. Orris, "Aerogel as a Soft Acoustic Metamaterial for Airborne Sound", Phys. Rev. Appl. **5**, 034012 (2016).
- [8] Z. Yang, J. Mei, M. Yang, N. H. Chan and P. Sheng, "Membrane-Type Acoustic Metamaterial with Negative Dynamic Mass", Phys. Rev. Lett. **101**, 204301 (2008).
- [9] V. Romero-García, G. Theocharis, O. Richoux, A. Merkel, V. Tournat and V. Pagneux, "Perfect and broadband acoustic absorption by critically coupled sub-wavelength resonators", Sci. Rep. **6**, 19519 (2016).
- [10] G. Ma, M. Yang, S. Xiao, Z. Yang and P. Sheng, "Acoustic metasurface with hybrid resonances", Nat. Mat. **13**, 873-878 (2014).
- [11] S.H. Lee, C.M. Park, Y.M. Seo, Z.G. Wang and C.K. Kim, "Composite Acoustic Medium with Simultaneously Negative Density and Modulus", Phys. Rev. Lett. **104**, 054301 (2010).
- [12] J.Zhang, V. Romero-García, G.Theocharis, O.Richoux, V. Achilleos and D. J. Frantzeskakis, "Second-Harmonic Generation in Membrane-Type Nonlinear Acoustic Metamaterials", Crystals **6** (2016).
- [13] J.Zhang, V. Romero-García, G.Theocharis, O.Richoux, V. Achilleos and D. J. Frantzeskakis, "Bright and Gap Solitons in Membrane-Type Acoustic Metamaterials", Phys. Rev. E **96** (2017).
- [14] A.H. Alaoui, T. Woignier, G.W. Scherer, J. Phalippou, "Comparison between flexural and uniaxial compression tests to measure the elastic modulus of silica aerogel", J. Non-Cryst. Solids **354**, 4556-4561 (2008).
- [15] T. Woignier, J. Pelous, J. Phalippou, R. Vacher and E. Courtens, "Elastic properties of silica aerogels", J. Non-Cryst. Solids **95&96**, 1197-1202 (1987).
- [16] T. Woignier and J. Phalippou "Mechanical strength of silica aerogels", J. Non-Cryst. Solids **100**, 404-408 (1988).
- [17] R. Haj-Ali, R. Eliasi, V. Fourman, C. Tzur, G. Bar, E. Grossman, R. Verker, R. Gvishi, I. Gouzman and N. Eliaz, "Mechanical characterization of aerogel materials with digital image correlation", Micropor. Mesopor. Mat. **226**, 44-52 (2016).
- [18] T.E. Gomez Alvarez-Arenas, F.R. Montero de Espinosa, M. Moner-Girona, E. Rodriguez, A. Roig and E. Molins, "Viscoelasticity of silica aerogels at ultrasonic frequencies", Appl. Phys. Lett. **81**, (2002).
- [19] J. Groby, T. Schlieff and J. Fricke "Ultrasonic evaluation of elastic properties of silica aerogels", Mater. Sci. Eng. **168**, 235-238, (1993).
- [20] V. Romero-García, G. Theocharis and V. Pagneux, O. Richoux, "Use of complex frequency plane to design broadband and sub-wavelength absorbers", J. Acoust. Soc. Am. **139**, 3395–3403 (2016).
- [21] K.F. Graff, "Wave Motion in Elastic Solids", Dover Publications New York, (1975).
- [22] B.H. Song, J.S. Bolton, "A transfer-matrix approach for estimating the characteristic impedance and wave numbers of limp and rigid porous materials", J. Acoust. Soc. Am. **107**, 1131 (2000).
- [23] M. R. Stinson "The propagation of plane sound waves in narrow and wide circular tubes, and generalization to uniform tubes of arbitrary crosssectional shape", J. Acoust. Soc. Am. **89**, 550-558 (1991).
- [24] M. Niskanen, J.-P. Groby, A. Duclos, O. Dazel, J. C. Le Roux, N. Poulain, T. Huttunen and T. Lahivaara "Deterministic and statistical characterization of rigid frame porous materials from impedance tube measurements", J. Acoust. Soc. Am. **142**, 2407-2418 (2017).
- [25] Y. Censor, "Pareto Optimality in Multiobjective Problems", Appl. Math. Optimiz. **4**, 41–59 (1977).
- [26] T. Back, "Selective pressure in evolutionary algorithms: a characterization of selection mechanisms", Proceedings of the First IEEE Conference on Evolutionary Computation, IEEE Press, Orlando, 57:62 (1994).
- [27] L Forest, V Gibiat, and T. Woignier, "Biot's theory of acoustic



- 461 propagation in porous media applied to aerogels and alcogels”,  
462 J. Non-Cryst. Solids, **225**, 287 (1998).
- 463 [28] J. Gross, G. Reichenauer, J. Fricke, “Mechanical properties of  
464 SiO<sub>2</sub> aerogels”, J. Phys. D **21**, 1447 (1988).
- 465 [29] N. Jiménez, W. Huang, V. Romero-García, V. Pagneux, J.-  
466 P. Groby “Ultra-thin metamaterial for perfect and quasi-  
467 omnidirectional sound absorption”, Appl. Phys. Lett. **109**,  
468 121902 (2016).
- 469 [30] N. Jiménez, V. Romero-García, V. Pagneux, J.-P. Groby  
470 “Rainbow-trapping absorbers: Broadband, perfect and asym-  
471 metric sound absorption by subwavelength panels for transmis-  
472 sion problems”, Sci. Rep. **7**, 13595 (2017).